

Design of New High Step up DC-DC Converter for Grid Connected System

T.Venkata Rao

M-Tech Student Scholar

Department of Electrical & Electronics Engineering,
Chirala Engineering College,
Chirala, Prakasam (Dt); Andhra Pradesh, India.

P.Bala Nagu

Associate Professor

Department of Electrical & Electronics Engineering,
Chirala Engineering College,
Chirala, Prakasam (Dt); Andhra Pradesh, India.

Abstract:

Recent trends in power conversion indicate a need for dc-dc power conversion at very high power levels and with high voltage buck/boost ratio for transmission/distribution purposes. No single conventional topology is well suited to these constraints. This paper presents a New Bidirectional DC-DC converter with high conversion ratio. The proposed converter uses the coupled-inductor to achieve high voltage conversion ratio. In the boost mode, the proposed converter is cascaded by boost converter and fly back converter with voltage double to increase the voltage gain. The switch voltage stress is reduced by a voltage clamping circuit, and the leakage-inductor energy is recycled. In the buck mode, the circuit consists of asymmetrical half-bridge fly back converter and buck converter. The leakage-inductor energy is recycled by a clamping circuit, and all of the switches achieve zero-voltage-switching turn on.

This paper first analyzes the proposed converter operating principles and steady-state circuit characteristics. Eventually, a Simulation circuit with conversion voltage 24 V/400 V and output power 500 W is implemented to verify the feasibility of the proposed converter. In step-up mode, the primary and secondary windings of the coupled inductor are operated in parallel charge and series discharge to achieve high step-up voltage gain. In step-down mode, the primary and secondary windings of the coupled inductor are operated in series charge and parallel discharge to achieve high step-down voltage gain. Thus, the proposed converter has higher step-up and step-down voltage gains than the conventional bidirectional DC-DC boost/buck converter.

Index Terms:

step-down and step-up, AC module, coupled inductor, PV cell.

I.INTRODUCTION:

Nowadays, renewable energy is increasingly valued and employed worldwide because of energy shortage and environmental contamination [1]–[4].

Renewable energy systems generate low voltage output, and thus, high step-up dc/dc converters have been widely employed in many renewable energy applications such as fuel cells, wind power generation, and photovoltaic (PV) systems. Such systems transform energy from renewable sources into electrical energy and convert low voltage into high voltage via a step-up converter, which can convert energy into electricity using a grid inverter. Fig. 1 shows a typical renewable energy system that consists of renewable energy sources, a step-up converter, and an inverter for ac application. The high step-up conversion may require two-stage converters with cascade structure for enough step-up gain, which decreases the efficiency and increases the cost. Thus, a high step-up converter is seen as an important stage in the system because such a system requires a sufficiently high step-up conversion with high efficiency [5]. Theoretically, conventional step-up converters, such as the boost converter and flyback converter, cannot achieve a high step-up conversion with high efficiency because of the resistances of elements or leakage inductance; also, the voltage stresses are large.

Thus, in recent years, many novel high step up converters have been developed [6]–[8]. Despite these advances, high step-up single-switch converters are unsuitable to operate at heavy load given a large input current ripple, which increases conduction losses. The conventional boost converter is an excellent candidate for high-power applications and power factor correction. Unfortunately, the step-up gain is limited, and the voltage stresses on semiconductor components are equal to output voltage. Hence, based on the aforementioned considerations, modifying a conventional boost converter for high step-up and high-power application is a suitable approach. To integrate switched capacitors into a boost converter may make voltage gain reduplicate, but no employment of coupled inductors causes the step-up voltage gain to be limited [9], [10]. Oppositely, to integrate only coupled inductors into a boost converter may make voltage gain higher and adjustable, but no employment of switched capacitors causes the step-up voltage gain to be ordinary. Thus, the synchronous employment of coupled inductors and switched capacitors is a better concept; moreover, high step-up gain, high efficiency, and low voltage stress are achieved even for high-power applications [11].

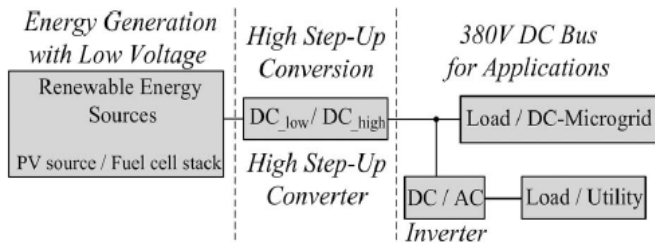


Fig. 1. Typical renewable energy system.

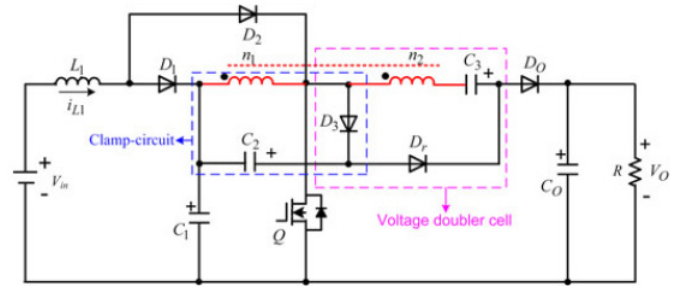
Many boost converters based on a coupled inductor or tapped inductor provide solutions to achieve a high voltage gain, and low voltage stress on the active switch without the penalty of high duty ratio. However, the input current is not continuous. Particularly, as the turn ratio of the coupled inductor or tapped inductor is increased to extend the voltage conversion ratio, the input current ripple becomes larger. Thereby, an input filter is inserted into a coupled-inductor boost converter. In order to satisfy the extremely high step-up applications and low input current ripple, a cascaded high step-up converter with an individual input inductor was proposed [12], which can be divided as a basic boost converter and a boost-flyback converter.

In this paper, a novel single switch dc–dc converter with high voltage gain is presented. The features of the proposed converter are as follows: 1) the voltage gain is efficiently increased by a coupled inductor and the secondary winding of the coupled inductor is inserted into a diode-capacitor for further extending the voltage gain dramatically; 2) a passive clamped circuit is connected to the primary winding of the coupled inductor to clamp the voltage across the active switch to lower voltage level. As a result, the power devices with low voltage rating and low on-state resistance RDS (ON) can be selected. On the other hand, this diode–capacitor circuit is useful to increase voltage conversion ratio; 3) the leakage inductance energy of coupled inductor can be recycled, improving the efficiency; and 4) the potential resonance between the leakage inductance and the junction capacitor of output diode may be cancelled [13]-[16].

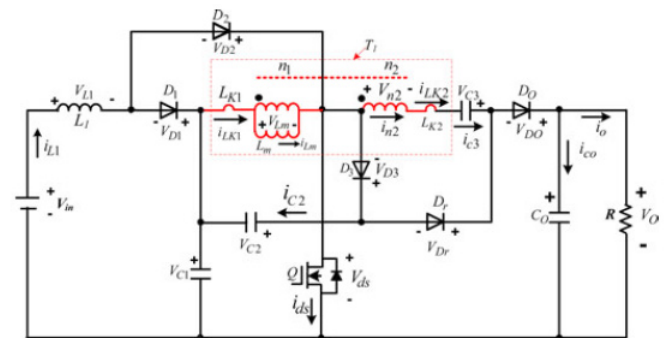
II. OPERATING PRINCIPLES OF THE PROPOSED CONVERTER:

Fig. 2(a) shows the circuit structure of the proposed converter, which consists of an active switch Q, an input inductor L1 and a coupled inductor T1, diodes D1, D2, and DO, a storage energy capacitor C1 and a output capacitor CO, a clamped circuit including diode D3 and capacitor C2, an extended voltage doubler cell comprising regeneration diode Dr and capacitor C3, and the secondary side of the coupled inductor [17]. The simplified equivalent circuit of the proposed converter is shown in Fig. 2(b).

The dual-winding coupled inductor is modeled as an ideal transformer with a turn ratio $N (n_2 / n_1)$, a parallel magnetizing inductance L_m , and primary and secondary leakage inductance L_{k1} and L_{k2} .



(a)



(b)

Fig. 2. Circuit configuration of proposed converter.

In order to simplify the circuit analysis of the converter, some assumptions are as follows:

- 1) the input inductance L1 is assumed to be large enough so that i_{L1} is continuous; every capacitor is sufficiently large, and the voltage across each capacitor is considered to be constant during one switching period;

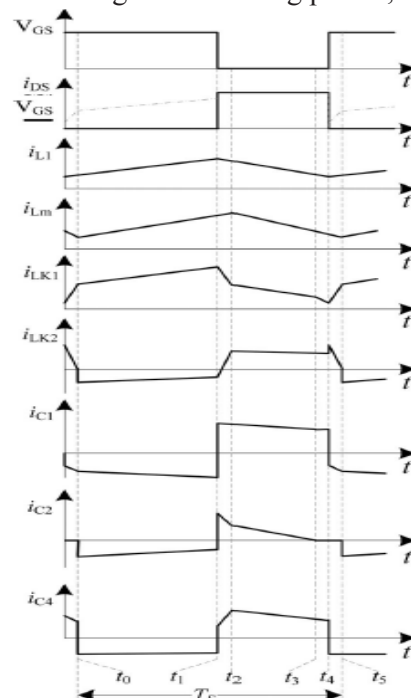


Fig. 3. The key waveforms of the proposed converter at C-CCM operation.

- 2) All components are ideal except the leakage inductance of the coupled inductor;
- 3) Both inductor currents i_{L1} and i_{Lm} are operated in continuous conduction mode, which is expressed as C-CCM; the inductor current i_{L1} is operated in continuous conduction mode, but the current i_{Lm} of the coupled inductor is operated in discontinuous conduction mode, which is called C-DCM.

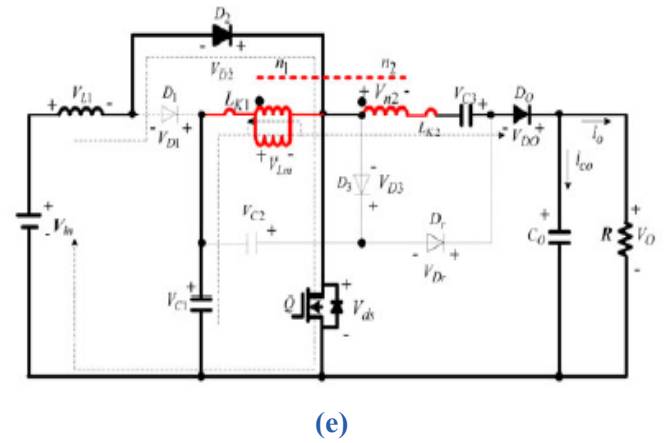
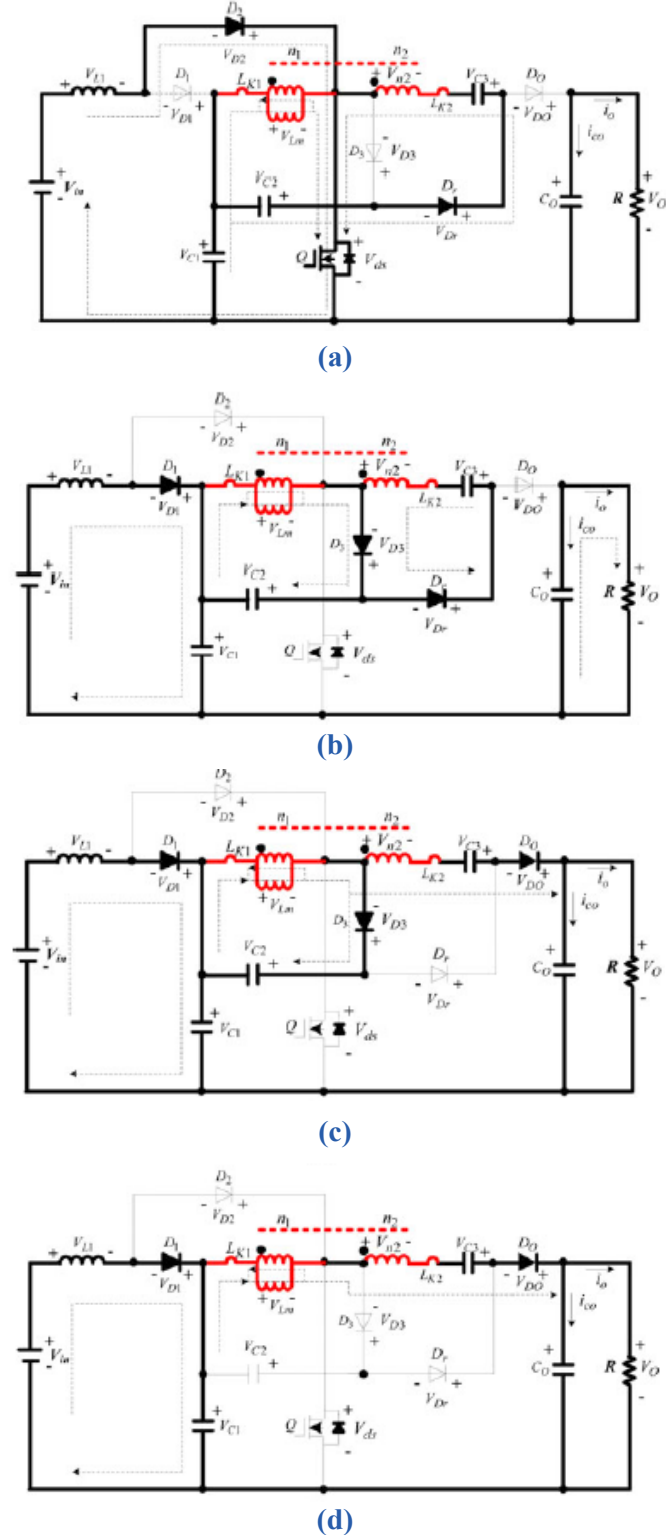


Fig. 4 Equivalent circuits of five operating stages during one switching period at C-CCM operation.

A.C-CCM:

Based on the aforementioned assumption, Fig. 3 illustrates some key waveforms under C-CCM operation in one switching period, and the corresponding equivalent circuits are shown in Fig. 4. The operating stages are described as follows:

1) Stage 1 $[t_0 -t_1]$: The switch Q is conducting at $t = t_0$. Diodes D_1, D_3 , and D_0 are reverse-biased by V_{C1} , $V_{C1}+V_{C2}$ and $V_O - V_{C1} - V_{C2}$, respectively. Only Diodes D_2 and D_r are turned ON. Fig. 4(a) shows the current-flow path. The dc source V_{in} energy is transferred to the inductor L_1 through D_2 and Q. Therefore, the current i_{L1} is increasing linearly. The primary voltage of the coupled inductor including magnetizing inductor L_m and leakage L_{k1} is V_{C1} and the capacitor C_1 is discharging its energy to the magnetizing inductor L_m and primary leakage inductor L_{k1} through Q. Then currents i_{D2} , i_{Lm} , and i_{k1} are increasing. Meanwhile, the energy stored in C_2 and C_1 is released to C_3 through D_r . The load R energy is supplied by the output capacitor C_0 . This stage ends at $t = t_1$.

2) Stage 2 $[t_1 -t_2]$: In this transition interval, Fig. 4(b) depicts the current-flow path of this stage. Once Q is turned OFF at $t = t_1$, the current through Q is forced to flow through D_3 . At the same time, the energy stored in inductor L_1 flows through diode D_1 to charge capacitor C_1 instantaneously and the current i_{L1} declines linearly. Thus, the diode D_2 is reverse biased by V_{C2} . The diode D_0 is still reverse biased by $V_O - V_{C1} - V_{C2}$. The energy stored in inductor L_{k1} flows through diode D_3 to charge capacitor C_2 . Therefore, the energy stored in L_{k1} is recycled to C_2 . The i_{Lk2} keeps the same current direction for charging capacitor C_3 through diode D_3 and regeneration-diode D_r . The voltage stress across Q is the summation of V_{C1} and V_{C2} . The load energy is supplied by the output capacitors C_0 . This stage ends when i_{Lk2} reaches zero at $t = t_2$.

3) Stage 3 [t₂–t₃]: During this transition interval, switch Q remains OFF. Since i_{LK2} reaches zero at t = t₂, VC₂ is reflected to the secondary side of coupled inductor T₁; thus, regeneration-diode Dr is blocked by VC₃ + NVC₂. Meanwhile, the diode D_O starts to conduct. Fig. 4(c) depicts the current-flow path of this stage. The inductance L₁ is still releasing its energy to the capacitor C₁. Thus, the current i_{L1} still declines linearly. The energy stored in L_{k1} and L_m is released to C₂. Moreover, the energy stored in L_m is released to the output via n₂ and C₃. The leakage inductor energy can thus be recycled, and the voltage stress of the main switch is clamped to the summation of VC₁ and VC₂. This stage ends when current i_{LK1} = i_{LK2}, thus the current i_{C2} = 0 at t = t₃.

4) Stage 4 [t₃ –t₄]: During this time interval, the switch Q, diodes D₂ and Dr is still turned OFF. Since i_{C2} reaches zero at t = t₃, the entire current of i_{LK1} flows through D₃ is blocked. The current-flow path of this mode is shown in Fig. 4(d). The energy stored in an inductor L₁ flows through diode D₁ to charge capacitor C₁ continually, so the current i_{L1} is decreasing linearly. The dc source V_{in}, L₁, L_m, L_{k1}, the winding n₂, L_{k2} and VC₃ are series connected to discharge their energy to capacitor C_o and load R. This stage ends when the switch Q is turned ON at t = t₄.

5) Stage 5 [t₄ –t₅]: The main switch Q is turned ON at t₄. During this transition interval, diodes D₁, D₃, and Dr are reverse-biased by VC₁, VC₁+VC₂ and V_O – VC₁ – VC₂, respectively. Since the currents i_{L1} and i_{Lm} are continuous, only diodes D₂ and D_O are conducting. The current-flow path is shown in Fig. 4(e). The inductance L₁ is charged by input voltage V_{in}, and the current i_{L1} increases almost in a linear way. The blocking voltages VC₁ is applied on magnetizing inductor L_m and primary-side leakage L_{k1}, so the current i_{Lk1} of the coupled inductor is increased rapidly. Meanwhile, the magnetizing inductor L_m keeps on transferring its energy through the secondary winding to the output capacitor C_O and load R. At the same time, the energy stored in C₃ is discharged to the output. Once the increasing i_{LK1} equals the decreasing current i_{Lm} and the secondary leakage inductor current i_{k2} declines to zero at t = t₅, this stage ends.

B.C-DCM:

To simplify the C-DCM analysis, all leakage inductances of the coupled inductor are neglected. The coupled inductor is modeled as a magnetizing inductor L_m and an ideal transformer. The key waveforms of the proposed converter are shown in Fig. 5. There are four main stages during one switching cycle. The equivalent circuits for each subinterval are shown in Fig. 6.

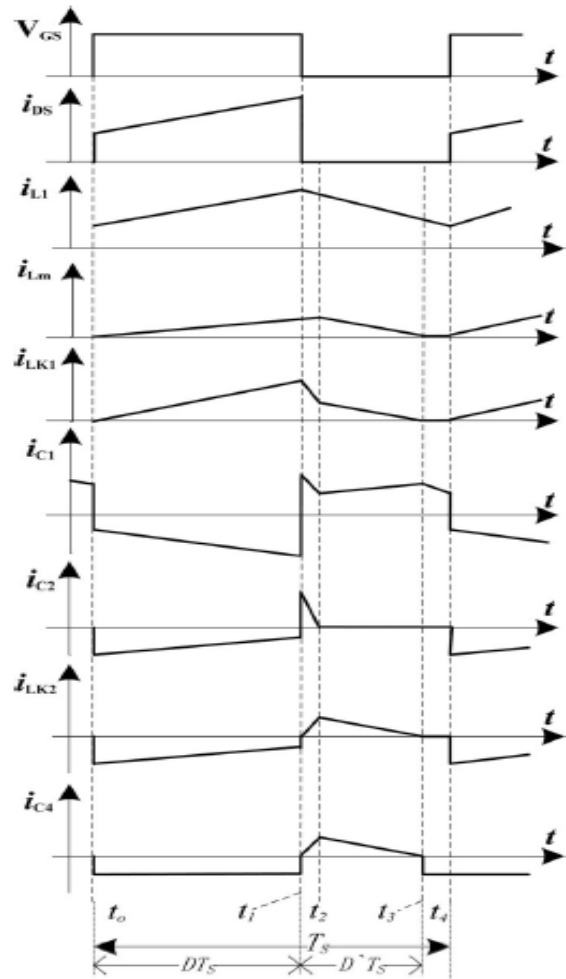
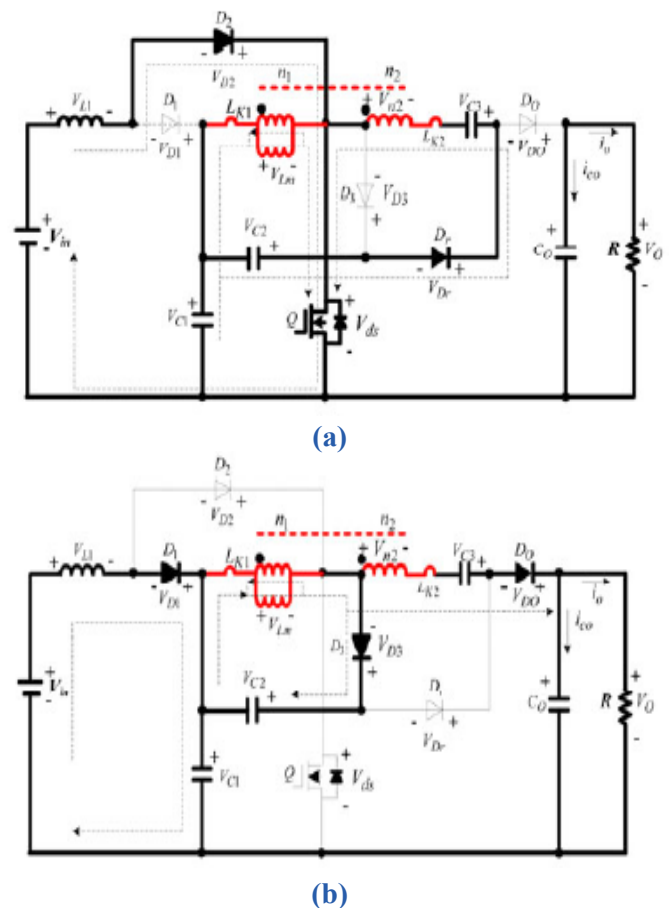


Fig. 5. The key waveforms of the proposed converter at C-DCM operation.



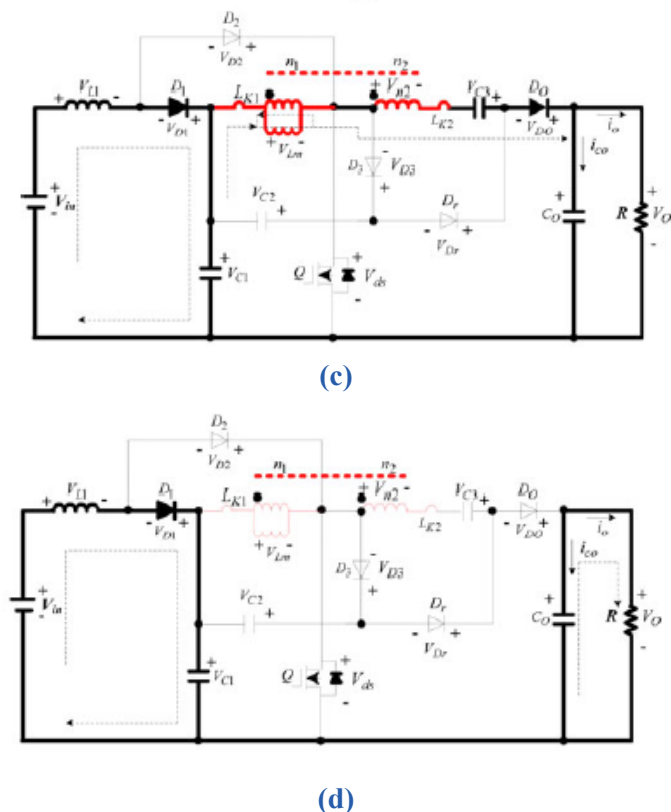


Fig. 6. Equivalent circuits of four operating stages during one switching period at DCM operation.

The detailed operation of each case is presented next.

1) Stage 1 [t0 –t1]: During this time interval, Q is turned ON. Diodes D2 and Dr are conducted but diodes D1, D3, and D0 are blocked by VC1, VC1+VC 2 , and VO – VC1 – VC2 , respectively. The current-flow path is shown in Fig. 6(a). The inductance L1 is charged by input voltage Vin; thus, the current iL1 increases linearly. The energy from capacitor C1 transfers to magnetizing Lm and current iLm increases linearly. Meanwhile, capacitor C3 is charged through the secondary winding coil n2 by capacitors C1 and C2. The output capacitor CO provides its energy to load R. The clamped diodeD3 is biased forward when the main switch Q is turned OFF at t = t1 , and this stage ends.

2) Stage 2 [t1–t2]: At t = t1 , the switch Q is turned OFF, resulting in a current commutation between the switch Q and diode D3 immediately. During this transition time interval, diodes D2 and Dr are turned OFF because they are respectively anti biased by VC2 and VO – VC1 – VC2 , and other diodes are conducting. The current-flow path is shown in Fig. 6(b). The dc sources Vin is series-connected with inductor L1 and transfer their energies to the capacitor C1 through D1 . The capacitors C2 is charged by the magnetizing inductor Lm via D3 . Similarly, the dc source Vin , inductor L1, magnetizing inductor Lm and capacitor C3 are series connected to transfer their energy to capacitor Co and load R. This stage ends when the rising current iC3 equals to current iLm at t = t2 . At the same instant, the diode D3 is reverse biased at t = t2 .

3) Stage 3 [t2 –t3]: During this time interval, the switch Q, D2 and Dr remain turned OFF. The diodes D1 and D0 are still turned ON. Since iC2 reaches zero at t2 , the coupled inductor transfers energy to the output, and diode D3 is also blocked. The current-flow path is shown in Fig. 6(c). The dc source Vin and the input inductor L1 are still connected serially to charge capacitor C1 . Thus, the current iL1 continues to decrease. Meantime, the primary and secondary sides of doubled-inductor are serially connected, and serially connected with VC3 , delivering their energy to the output capacitor CO and load R. This stage ends when the current iLm reduces to zero at t = t3 .

4) Stage 4 [t3 –t4]: During this transition time interval, the switch Q and the diode D2 is still turned OFF. Meanwhile, the primary and secondary currents of the coupled inductor have run dry at t3 . Therefore, the diode D3 is still blocked by VC1+VC 2 , and only diode D1 is conducting for continuous iL1 . The current-flow path is shown in Fig. 6(d). The capacitor C1 is still charged by the energy stored in L1 and dc sources Vin . Since the energy stored in Lm is empty, the energy stored in CO is discharged to load R. This stage ends when Q is turned ON at t = t4 , which is the beginning of the next switching period.

III. STEADY-STATE ANALYSIS OF PROPOSED CONVERTERS:

A.C-CCM Operating Conduction:

To simplify the analysis, the leakage inductances of the coupled inductor are neglected in the steady-state analysis. Also, the losses of the power devices are not considered. Only stages 1 and 3 are considered for C-CCM operation because the time durations of stages 2, 4, and 5 are short significantly. At stage1, the main switch Q is turned ON, the inductor L1 is charged by the input dc source Vin , and the magnetizing inductor Lm is charged by the voltage across C1 . The following equations can be written from Fig. 4(a):

$$V_{L1} = V_{in} \tag{1}$$

$$V_{Lm} = V_{C1}. \tag{2}$$

And the voltage of the switched capacitor C3 can be expressed by

$$V_{C3} = NV_{C1} + V_{C1} + V_{C2}. \tag{3}$$

During stage 3, the main switch Q is in the OFF state, the inductor L1 and magnetizing inductor Lm are discharged, respectively. The voltages across the inductor L1 and Lm can be obtained by

$$V_{L1} = V_{in} - V_{C1} \tag{4}$$

$$V_{Lm} = -V_{C2} \tag{5}$$

$$V_o = V_{C1} + (N + 1)V_{C2} + V_{C3}. \quad (6)$$

Using the inductor volt-second balance principle to the inductor $L1$ and magnetizing inductor Lm , the following equations can be expressed as:

$$\int_0^{DT_s} V_{in} dt + \int_{DT_s}^{T_s} (V_{in} - V_{C1}) dt = 0 \quad (7)$$

$$\int_0^{DT_s} V_{C1} dt + \int_{DT_s}^{T_s} (-V_{C2}) dt = 0. \quad (8)$$

From (1)–(8), the voltages across capacitors $C1$, $C2$, and $C3$ are derived as follows:

$$V_{C1} = \frac{V_{in}}{1 - D} = \frac{(1 - D)V_o}{2 + N} \quad (9)$$

$$V_{C2} = \frac{D \cdot V_{in}}{(1 - D)^2} = \frac{DV_o}{2 + N} \quad (10)$$

$$V_{C3} = \frac{(N + 1 - DN)V_{in}}{(1 - D)^2} = \frac{(N + 1 - DN)V_o}{2 + N}. \quad (11)$$

Substituting (9)–(11) into (6), the dc voltage gain MC-CCM is obtained as

$$M_{C-CCM} = \frac{V_o}{V_{in}} = \frac{(2 + N)}{(1 - D)^2}. \quad (12)$$

B.C-DCM Operating Condition:

In C-DCM operation, there are four stages. The key waveforms are shown in Fig. 5. During the time of stage 1, the switch Q is turned ON, and only diodes $D2$ and Dr are turned ON. The following equations can be written as:

$$V_{L1} = V_{in}$$

$$V_{Lm} = V_{C1}$$

$$V_{n2} = NV_{Lm} = V_{C3} - V_{C2} - V_{C1}.$$

During the time of stage 3, the switch Q is turned OFF, and only diodes $D1$ and $D0$ are conducting. The voltage levels across inductor $L1$ and magnetizing Lm and the secondary winding coil $n2$ are given as follows:

$$V_{L1} = V_{in} - V_{C1}$$

$$V_{Lm} = \frac{V_{C3} + V_{C1} - V_o}{N + 1}$$

$$V_{n2} = \frac{N(V_{C3} + V_{C1} - V_o)}{N + 1}.$$

During the time of stage 2, the output voltage V_o can be expressed as

$$V_o = V_{C1} + V_{C3} + (N + 1)V_{C2}.$$

If $D_$ is defined as the duty cycle of the magnetizing inductor current from peak point ramped down to zero. By applying the volt-second balance principle to the inductor $L1$, magnetizing inductor Lm and the secondary side of winding coil $n2$, the following equations are derived:

$$\int_0^{DT_s} V_{in} dt + \int_{DT_s}^{(D+D')T_s} (V_{in} - V_{C1}) dt = 0$$

$$\int_0^{DT_s} V_{C1} dt + \int_{DT_s}^{(D+D')T_s} \frac{V_{C3} + V_{C1} - V_o}{N + 1} dt = 0$$

$$\int_0^{DT_s} (V_{C3} - V_{C1} - V_{C2}) dt + \int_{DT_s}^{(D+D')T_s} \times \frac{N(V_{C3} + V_{C1} - V_o)}{N + 1} dt = 0.$$

The voltages of $C1$, $C2$, $C3$, and $D_$ are obtained

$$V_{C1} = \frac{V_{in}}{1 - D}$$

$$V_{C2} = \frac{D \cdot V_{in}}{(1 - D)D'}$$

$$V_{C3} = \frac{[(N + 1)D' + D]V_{in}}{(1 - D)D'}$$

$$M_{C-DCM} = \frac{V_o}{V_{in}} = \frac{(2 + N)(D' + D)}{(1 - D)D'}$$

IV. Grid connected converters:

The use of power electronic converters as interface to power sources, energy storages and power consumers will increase. One application example is autonomous power systems where renewable energy sources like wind and fuel cells are integrated with appropriate storage elements to gain energy efficient and reliable energy supply. Other examples are ship electric propulsion systems, electric cars/buses and autonomous power systems of ships, offshore installations and remote utility networks..

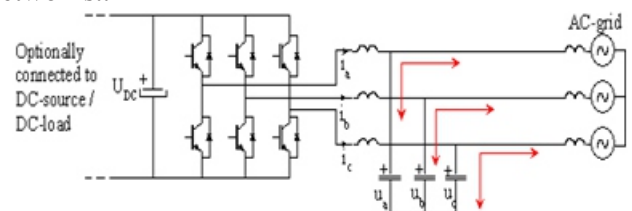


Fig.7. Block diagram representation of grid connected system

The performance of a grid-connected AC-converter that interfaces a DC-power source to the grid has a lot more controllability than a traditional synchronous generator. The designer of the converter has therefore the possibility to select the behavior of the converter during and after a transient or a line fault. A converter can for example change its reactive power flow almost instantly. The system components of existing AC-grids, including protection relays, are usually designed assuming synchronous generators as power sources. It is therefore important to verify that alternative converter interfaced power sources are compatible to the existing system in normal operation, but also during faults and transients.

The importance of suitable simulation tools, modeling techniques and laboratory facilities then becomes apparent (see results summaries for the activities simulation and modeling and energy laboratory).

V.MATLAB MODELING AND SIMULATION RESULTS:

A prototype sample is presented to verify using MATLAB/SIMULINK Platform to the practicability of the proposed converter. Here simulation is carried out in two different cases 1) Implementation of Proposed Converter with constant DC Sources operated in CCM mode 2) Implementation of Proposed Converter applied to grid connected system.

Case 1: Implementation of proposed converter with boost mode:

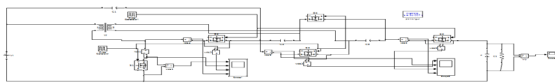


Fig. 8 shows the Matlab/Simulink Model of Proposed boost mode using Matlab/Simulink platform.

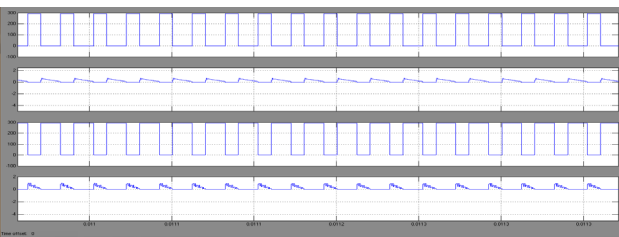
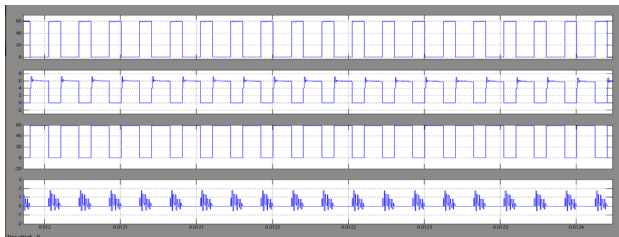


Fig.9 shows the Diode across Voltages & Switch across Voltage, capacitor currents, input inductor currents, output capacitor current of proposed boost converter.

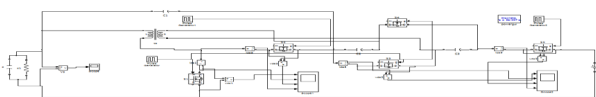


Fig. 10 shows the Matlab/Simulink Model of Proposed buck mode using Matlab/Simulink platform.

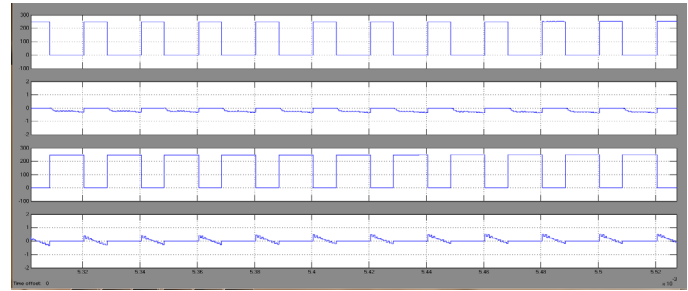


Fig.11 shows the Diode across Voltages & Switch across Voltage, capacitor currents, input inductor currents, output capacitor current of proposed boost converter.

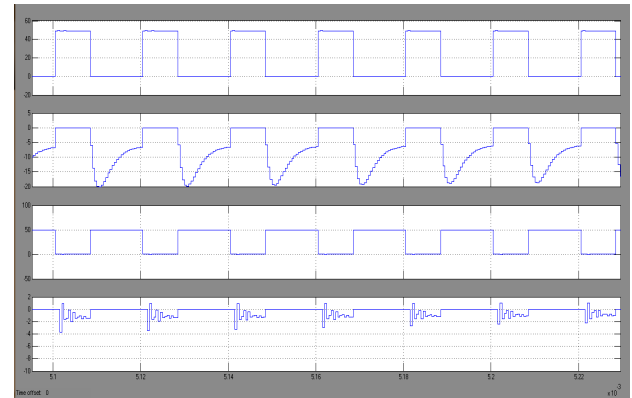


Fig.12 shows the Diode across Voltages & Switch across Voltage, capacitor currents, input inductor currents, output capacitor current of proposed boost converter.

Case 2: Implementation of Proposed Converter applied to grid connected system.

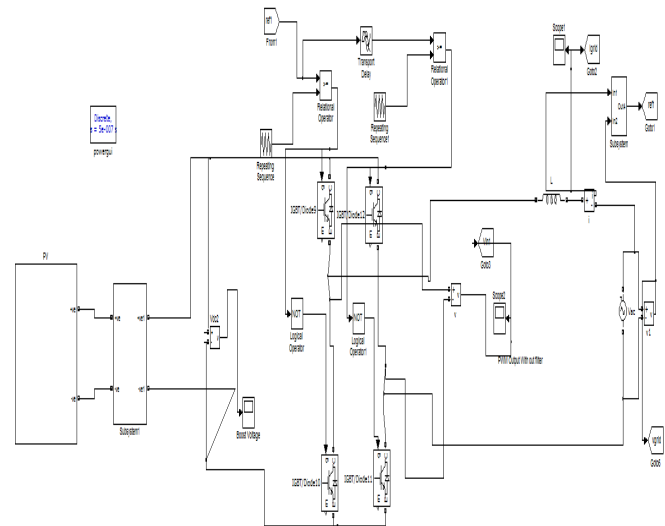


Fig. 13 Matlab/Simulink Model of Proposed High Step up DC/DC Converter with RES Interfaced to Grid.

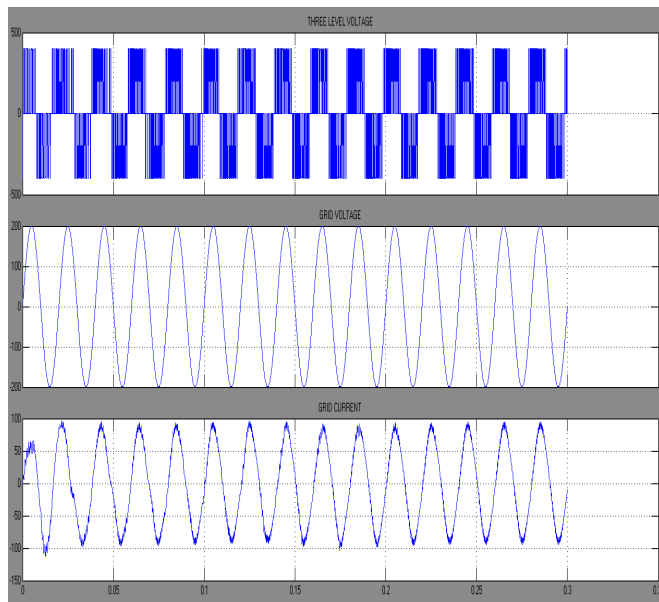


Fig.14 Three Level Output Voltage, Grid Voltage, Grid Current.

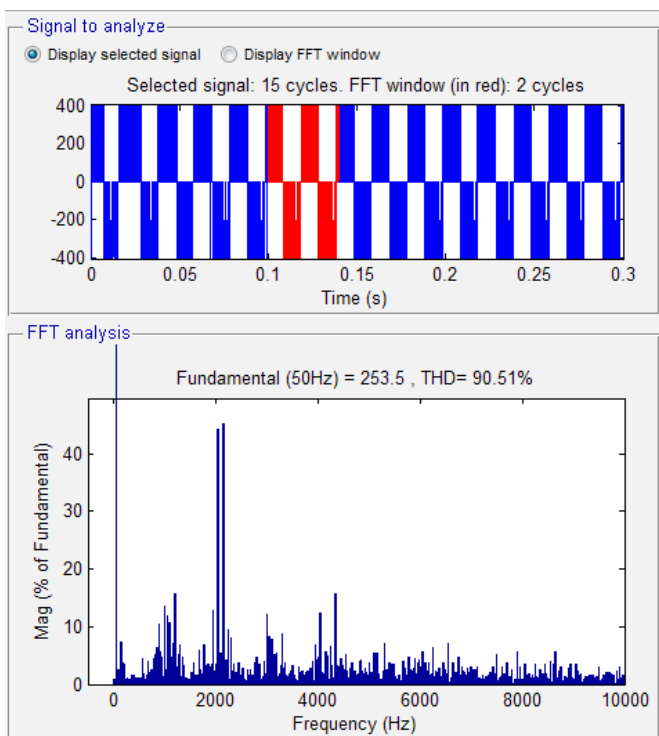


Fig.15 FFT Analysis of Inverter Voltage without filter.

Fig.16 FFT Analysis of Inverter Voltage without filter of Proposed High Step up DC/DC Converter with RES Interfaced to Grid.

VI.CONCLUSION:

The conventional energy sources, obtained from our environment, tend to exhaust with relative rapidity due to its irrational utilization by the humanity. Renewable energy offers a promising alternative source. Solar energy seems to be most attractive in present days. Power electronics applications requiring high-voltage high-power

converters have been steadily growing in fields such as interfacing RES system, power quality, power systems control, adjustable speed drives, and uninterruptible power supplies (UPS), and co-generation. Most applications demand high voltage gain converters. Various converter topologies have been proposed in the literature, to improve performance, adapt to requirements and avoid proprietary technologies. This paper proposes the non-isolated high step-up industry applications, a novel high-voltage gain converter is introduced in this paper, which combines a quadratic boost converter with coupled inductor and diode-capacitor techniques. A clamped-capacitor circuit is connected to the primary side of the coupled inductor, the voltage stress of the active switch is reduced greatly and the clamped capacitor also transfers the primary leakage energy to the output. At last same converter applied to grid connected system by using three level inverter topology and results are presented.

REFERENCES:

- [1] J F. Boico, B. Lehman, and K. Shujaee, "Solar battery chargers for NiMH batteries," *IEEE Trans. Power Electron.*, vol. 26, no. 5, pp. 1600–1609, Sep. 2007.
- [2] M. Prudente, L. L. Pfitscher, G. Emmendoerfer, E. F. Romaneli, and R. Gules, "Voltage multiplier cells applied to non-isolated DC-DC converters," *IEEE Trans. Power Electron.*, vol. 23, no. 2, pp. 871–887, Mar.2008.
- [3] H. Kanchev, D. Lu, F. Colas, V. Lazarov, and B. Francois, "Energy management and operational planning of a micro grid with a PV-based active generator for smart grid applications," *IEEE Trans. Ind. Electron.*, vol. 58, no. 10, pp. 4583–4592, Oct. 2011.
- [4] Q. Zhao and F. C. Lee, "High-efficiency, high step-up DC-DC converters," *IEEE Trans. Power Electron.*, vol. 18, no. 1, pp. 65–73, Jan. 2003.
- [5] A. Vaccaro, G. Velotto, and A. F. Zobaa, "A decentralized and cooperative architecture for optimal voltage regulation in smart grids," *IEEE Trans. Ind. Electron.*, vol. 58, no. 10, pp. 4593–4602, Oct. 2011.
- [6] L Yan and B Lehman, "An integrated magnetic isolated two-inductor boost converter: Analysis, design and experimentation," *IEEE Trans. Power Electron.*, vol. 20, no. 2, pp. 332–342, Jan. 2005.
- [7] Q Li and P Wolfs, "A review of the single phase photovoltaic module integrated converter topologies with three different DC link configurations," *IEEE Trans. Power Electron.*, vol. 23, no. 3, pp. 1320–1333, May 2008.

- [8] A. Reatti, "Low-cost high power-density electronic ballast for automotive HID lamp," *IEEE Trans. Power Electron.*, vol. 15, no. 2, pp. 361–368, Mar. 2000.
- [9] S. S. Lee, S. W. Choi, and G. O. Moon, "High efficiency active-clamp forward converter with transient current build-up (TCB) ZVS Technique," *IEEE Trans. Ind. Electron.*, vol. 54, no. 1, pp. 310–318, Feb. 2007.
- [10] E. S. da Silva, L. dos Reis Barbosa, J. B. Vieira, L. C. de Freitas, and V. J. Farias, "An improved boost PWM soft-single-switched converter with low voltage and current stresses," *IEEE Trans. Ind. Electron.*, vol. 48, no. 6, pp. 1174–1179, Dec. 2001.
- [11] H. S. H. Chung, W. C. Chow, S. Y. R. Hui, and S. T. S. Lee, "Development of a switched-capacitor DC–DC converter with bidirectional power flow," *IEEE Trans. Circuits Syst. I, Fund. Theory Appl.*, vol. 47, no. 9, pp. 1383–1389, Sep. 2000.
- [12] L. S. Yang, T. J. Liang, and J. F. Chen, "Transformerless dc–dc converters with high step-up voltage gain," *IEEE Trans. Ind. Electron.*, vol. 56, no. 8, pp. 3144–3152, Aug. 2009.
- [13] B. Axelrod, Y. Berkovich, and A. Ioinovici, "Switched-capacitor/ switched-inductor structures for getting transformerless hybrid DC–DC PWM converters," *IEEE Trans. Circuits Syst. I*, vol. 55, no. 2, pp. 687–696, Mar. 2008.
- [14] M. Zhu and F. L. Luo, "Series SEPIC implementing voltage-lift technique for DC–DC power conversion," *IET Power Electron.*, vol. 1, no. 1, pp. 109–121, Mar. 2008.
- [15] Y. Jang and M. M. Jovanovic, "Interleaved boost converter with intrinsic voltage-doubler characteristic for universal-line PFC front end," *IEEE Trans. Power Electron.*, vol. 22, no. 4, pp. 1394–1401, Jul. 2007.
- [16] L. S. Yang, T. J. Liang, H. C. Lee, and J. F. Chen, "Novel high step-up DC–DC converter with coupled-inductor and voltage-doubler circuits," *IEEE Trans. Ind. Electron.*, vol. 58, no. 9, pp. 4196–4206, Sep. 2011.
- [17] F. L. Luo, "Six self-lift dc–dc converters, voltage lift technique," *IEEE Trans. Ind. Electron.*, vol. 48, no. 6, pp. 1268–1272, Dec. 2001.
- [18] F. L. Tofoli, D. de Souza Oliveira, R. P. Torricobascop, and Y. J. A. Alcazar, "Novel non-isolated high-voltage gain DC–DC converters based on 3SSC and VMC," *IEEE Trans. Power Electron.*, vol. 27, no. 9, pp. 3897–3907, Sep. 2012.
- [19] J. W. Baek, M. H. Ryoo, T. J. Kim, D. W. Yoo, and J. S. Kim, "High boost converter using voltage multiplier," in *Proc. IEEE the 39th Annu. Conf. IEEE Ind. Electron. Society*, 2005, pp. 567–572.

Author's Profile:



Venkatarao Thammavarapu

Received B.Tech degree from QIS Engineering college, Ongole, Prakasam (dt), Andhra Pradesh. And currently pursuing M.Tech in Power Electronics at Chirala engineering college, Chirala, Prakasam(dt), Andhra Pradesh. His areas of interest are Power systems, Electrical Machines, and Power Electronics.



Bala Nagu Puppala

He received masters (M.tech-MECS) from VTU, Belgaum, Karnataka. Currently he is pursuing PHD (Power Systems) in JNTU Kakinada, Andhra Pradesh. He is working as an associate professor in Chirala Engineering College Chirala, Prakasam(dt), Andrapradesh.